

Synthesis, crystal structures, and magnetic properties of three pairs of chiral cyanide-bridged Fe(III)–Cu(II) enantiomeric complexes

Daopeng Zhang, Lingqian Kong, Hongyan Zhang & Kexun Chen

To cite this article: Daopeng Zhang, Lingqian Kong, Hongyan Zhang & Kexun Chen (2015) Synthesis, crystal structures, and magnetic properties of three pairs of chiral cyanide-bridged Fe(III)–Cu(II) enantiomeric complexes, *Journal of Coordination Chemistry*, 68:22, 3969-3981, DOI: [10.1080/00958972.2015.1080360](https://doi.org/10.1080/00958972.2015.1080360)

To link to this article: <http://dx.doi.org/10.1080/00958972.2015.1080360>



Accepted author version posted online: 13 Aug 2015.
Published online: 04 Sep 2015.



Submit your article to this journal [↗](#)



Article views: 73



View related articles [↗](#)



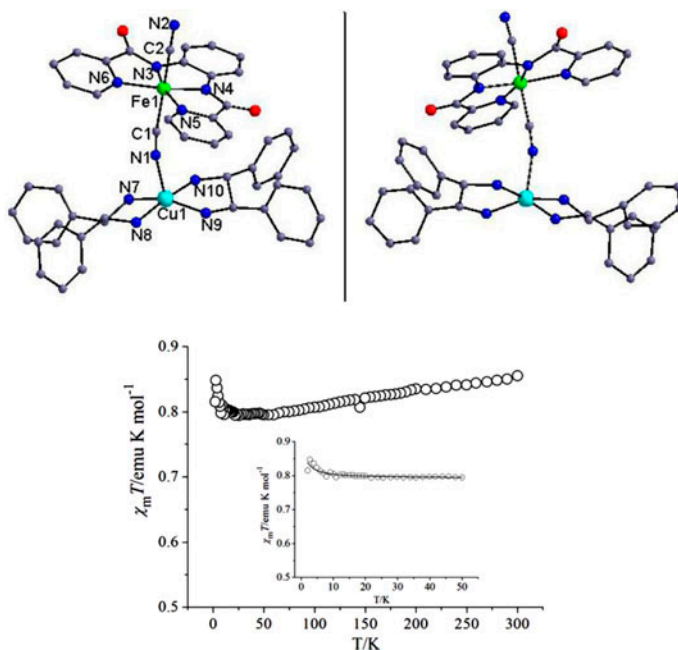
View Crossmark data [↗](#)

Synthesis, crystal structures, and magnetic properties of three pairs of chiral cyanide-bridged Fe(III)–Cu(II) enantiomeric complexes

DAOPENG ZHANG*[†], LINGQIAN KONG[‡], HONGYAN ZHANG[†] and
KEXUN CHEN*[†]

[†]College of Chemical Engineering, Shandong University of Technology, Zibo, PR China
[‡]Dongchang College, Liaocheng University, Liaocheng, PR China

(Received 16 February 2015; accepted 30 June 2015)



With three *trans*-dicyanideiron(III) precursors $K[Fe(L)(CN)_2]$ as building blocks ($L = bpb^{2-}$, $bpmb^{2-}$, $bpdmb^{2-}$; $bpb^{2-} = 1,2$ -bis(pyridine-2-carboxamido)-4,5-enzenate, $bpmb^{2-} = 1,2$ -bis(pyridine-2-carboxamido)-4-methylbenzenate, $bpdmb^{2-} = 1,2$ -bis(pyridine-2-carboxamido)-4,5-dimethylbenzenate) and two chiral copper(II) compounds $Cu[(S,S/R,R-dpen)_2](ClO_4)_2$ ($S,S/R,R-dpen = S,S/R,R,1,2$ -diphenylethylenediamine) as assembly segments, three pairs of cyanide-bridged enantiomers, $\{[(S,S/R,R-dpen)_2Cu(\mu-CN)Fe(bpb)(CN)]ClO_4\}_2$ (**1,2**), $\{[(S,S/R,R-dpen)_2Cu(\mu-CN)Fe(bpmb)(CN)]ClO_4\}_2$ (**3,4**), and $\{[(S,S/R,R-dpen)_2Cu(\mu-CN)Fe(bpdmb)(CN)]ClO_4\}_2$ (**5,6**), have been

*Corresponding authors. Email: dpzhang@sdtu.edu.cn (D. Zhang); kxch@sdtu.edu.cn (K. Chen)

obtained and characterized by elemental analysis, IR spectroscopy, and X-ray structure determination. Single X-ray diffraction analysis shows their similar binuclear structures, in which the cyanide-containing building blocks acting as a monodentate ligand through one of the two cyanide groups are linked to the five-coordinate Cu(II) ion, for which the four amine N complete the additional coordination positions. Investigation of magnetic properties of **1–6** reveals weak ferromagnetic magnetic exchange between the neighboring Fe(III) and Cu(II) ions through the bridging cyanide.

Keywords: Chiral; Cyanide-bridged; Crystal structure; Magnetic property

1. Introduction

Molecule-based materials exhibiting interesting magnetic behaviors, which include magnetic ordering with high ordering/critical temperatures (T_c), single molecule/chain quantum effects, magnetic state switching control via photo, thermal, pressure, etc. are hot topics because of their potential applications in magnetic devices [1–4]. As one of the most important magnetic systems, cyanide-bridged magnetic complexes have received attention due to their molecular topological structures, and magnetic coupling between neighboring metal ions through the cyanide bridge can be relatively readily controlled and predicted [5–7]. Many cyanide-bridged magnetic complexes with diverse structures and interesting magnetic properties have been synthesized [8–24].

To elucidate the magneto-structural correlation in low-dimensional magnetic system and to prepare interesting low-dimensional molecular materials such as single-molecule magnets and single-chain magnets, our group has developed a series of cyanide building blocks $[M(L)(CN)_2]^-$ ($M = Fe, Cr, Co$; $L =$ bpb derivatives, $bpb^{2-} = 1,2$ -bis(pyridine-2-carboxamido) benzenate) containing relatively large equatorial in-plane ligands and two *trans* cyanide groups [25–27], which have been good candidates for assembling low-dimensional cyanide-bridged heterometallic complexes. To throw further light on the reactions of $[Fe(L)(CN)_2]^-$ type cyanide precursors, and also to find new molecular materials with both magnetic properties and chirality using the appropriate chiral ancillary ligand for coordination with paramagnetic ions, we investigated the reactions of these types of precursors with chiral *S, S/R, R*-1,2-diphenylethylenediamine (*S, S/R, R*-dpen) copper compounds (scheme 1), the latter of which is being used for the first time to prepare cyanide-bridged magnetic complexes. In this article, we present our recent work which concerns the synthesis, crystal structures, and magnetic properties of six binuclear chiral cyanide-bridged Fe(III)–Cu(II) complexes $\{[(S/S\text{-dpen})_2Cu(\mu\text{-CN})Fe(bpb)(CN)]\}_2(ClO_4)_2 \cdot 2CH_3CN \cdot 1.5H_2O$ (**1**), $\{[(R/R\text{-dpen})_2Cu(\mu\text{-CN})Fe(bpb)(CN)]\}_2(ClO_4)_2 \cdot 2CH_3OH \cdot 2H_2O$ (**2**), $\{[(S/S\text{-dpen})_2Cu(\mu\text{-CN})Fe(bpmb)(CN)]\}ClO_4 \cdot CH_3CN \cdot CH_3OH \cdot 2H_2O$ (**3**), $\{[(R/R\text{-dpen})_2Cu(\mu\text{-CN})Fe(bpmb)(CN)]\}ClO_4 \cdot 4H_2O$ (**4**), $\{[(S/S\text{-dpen})_2Cu(\mu\text{-CN})Fe(bpMb)(CN)]\}ClO_4 \cdot CH_3CN \cdot CH_3OH \cdot 2H_2O$ (**5**), and $\{[(R/R\text{-dpen})_2Cu(\mu\text{-CN})Fe(bpMb)(CN)]\}ClO_4 \cdot CH_3CN \cdot CH_3OH \cdot 2H_2O$ (**6**).

2. Experimental

2.1. Physical measurements

Elemental analyses of carbon, hydrogen, and nitrogen were carried out with an Elementary Vario El. Infrared spectroscopy on KBr pellets was performed on a Magna-IR 750 spectrophotometer from 4000 to 400 cm^{-1} . Variable-temperature magnetic susceptibility and

field-dependent magnetization measurements were performed on a Quantum Design MPMS SQUID magnetometer. Crystals for **1**, **3**, and **5** were collected and used for magnetic measurement, and all samples with mass about 15–20 mg were placed in gelatine capsules held within a plastic straw. The experimental susceptibilities were corrected for the diamagnetism of the constituent atoms (Pascal's tables).

2.2. General procedures and materials

All the reactions were carried out in air and all chemicals and solvents used were reagent grade without purification. $\text{K}[\text{Fe}^{\text{III}}(\text{bpb})(\text{CN})_2]$ [bpb^{2-} = 1,2-bis (pyridine-2-carboxamido) benzenate] and its analogs were synthesized as described [28].

Caution! KCN is hypertoxic and hazardous. Perchlorate salts of metal complexes with organic ligands are potentially explosive. They should be handled in small quantities with care.

2.3. Preparation of 1–6

All six complexes were prepared using similar procedure. Therefore, only the preparation of **1** and **2** as representative are described in detail.

Complex 1. The acetonitrile solution (10 mL) formed *in situ* by $[\text{Cu}(\text{ClO}_4)_2] \cdot 6\text{H}_2\text{O}$ (36.5 mg, 0.1 mmol) and S,S-1,2-diphenylethylenediamine (42.4 mg, 0.2 mmol) was added slowly to a solution containing $\text{K}[\text{Fe}(\text{bpb})(\text{CN})_2]$ (93 mg, 0.20 mmol) dissolved in methanol (10 mL). The mixture was stirred only for 1 min at room temperature and filtered at once to remove any insoluble material, and then the filtrate was allowed to evaporate slowly without disturbance for 1 week. The dark-brown crystals suitable for X-ray diffraction were collected by filtration, washed with cool methanol, and dried in air. Yield: 53.2 mg, 49.7%. Anal. Calcd for $\text{C}_{100}\text{H}_97\text{Cl}_2\text{Cu}_2\text{Fe}_2\text{N}_{22}\text{O}_{13.5}$: C, 56.31; H, 4.58; N, 14.45. Found: C, 56.21; H, 4.47; N, 14.51. Main IR bands (cm^{-1}): 2160, 2127 (s, $\nu\text{C}\equiv\text{N}$), 1100 (vs., $\nu\text{Cl}=\text{O}$).

Complex 2. The procedure is almost same with that for the complex **1** except that using R, R-1,2-diphenylethylenediamine to replace S,S-1,2-diphenylethylenediamine. Yield: 55.1 mg, 51.9%. Anal. Calcd for $\text{C}_98\text{H}_{100}\text{Cl}_2\text{Cu}_2\text{Fe}_2\text{N}_{20}\text{O}_{16}$: C, 55.43; H, 4.75; N, 13.19. Found: C, 55.33; H, 4.62; N, 13.38. Main IR bands (cm^{-1}): 2161, 2127 (s, $\nu\text{C}\equiv\text{N}$), 1098 (vs., $\nu\text{Cl}=\text{O}$).

Complex 3. Yield: 56.9 mg, 48.5%. Anal. Calcd for $\text{C}_{52}\text{H}_{57}\text{ClCuFeN}_{11}\text{O}_9$: C, 55.03; H, 5.06; N, 13.58. Found: C, 54.87; H, 4.89; N, 13.79. Main IR bands (cm^{-1}): 2158, 2130 (s, $\nu\text{C}\equiv\text{N}$), 1100 (vs., $\nu\text{Cl}=\text{O}$).

Complex 4. Yield: 59.7 mg, 54.4%. Anal. Calcd for $\text{C}_{49}\text{H}_{54}\text{ClCuFeN}_{10}\text{O}_{10}$: C, 53.61; H, 4.96; N, 12.76. Found: C, 53.47; H, 4.81; N, 12.93. Main IR bands (cm^{-1}): 2161, 2128 (s, $\nu\text{C}\equiv\text{N}$), 1100 (vs., $\nu\text{Cl}=\text{O}$).

Complex 5. Yield: 59.6 mg, 51.9%. Anal. Calcd for $C_{53}H_{59}ClCuFeN_{11}O_9$: C, 55.40; H, 5.18; N, 13.41. Found: C, 55.27; H, 5.03; N, 13.55. Main IR bands (cm^{-1}): 2160, 2125 (s, $\nu C\equiv N$), 1100 (*vs.*, $\nu Cl=O$).

Complex 6. Yield: 71.6 mg, 62.3%. Anal. Calcd for $C_{53}H_{59}ClCuFeN_{11}O_9$: C, 55.40; H, 5.18; N, 13.41. Found: C, 55.30; H, 5.04; N, 13.57. Main IR bands (cm^{-1}): 2160, 2125 (s, $\nu C\equiv N$), 1098 (*versus*, $\nu Cl=O$).

2.4. X-ray data collection and structure refinement

Single crystals of all the complexes for X-ray diffraction analyses with suitable dimensions were mounted on a glass fiber, and the crystal data were collected on a Bruker APEX2 CCD area-detector with a MoK α sealed tube ($\lambda = 0.71073 \text{ \AA}$) at 293 K [29], using an ω scan mode. SAINT [29] was used for cell refinement and data reduction, and absorption correction was carried out with SADABS [30]. The structures were solved by direct methods and expanded using Fourier difference techniques with the SHELXTL-97 program package [31]. The nonhydrogen atoms were refined anisotropically, while hydrogens were introduced as fixed contributors. All of the nonhydrogen atoms were refined with anisotropic displacement coefficients. Hydrogens were assigned isotropic displacement coefficients $U(H) = 1.2U(C)$ or $1.5U(C)$, and their coordinates were allowed to ride on their respective carbons using SHELXL97, except some hydrogens of the solvent molecules. These were refined isotropically with fixed U values and appropriate DFIX commands were used to rationalize the bond parameter. There is some unresolved disorder in portions of the solvent/anion atoms, such as O2, O5, O6, O14 in **1**; O9, O10, O14 in **2**; O5, O8, O9 in **3**; O4, O5, O8, O9, O11 in **4**; O5, O8, O9 in **5**; O3, O4, O6, O7, O8, O9 in **6**, respectively. However, attempts to resolve the disorder in the refinement did not lead to improvement in the refinement. Details of the crystal parameters, data collection, and refinement are summarized in table 1.

3. Results and discussion

3.1. Synthesis and general characterization

A series of recent works [25–27] have shown that *trans*-dicyanometalate types of building blocks were good candidates for synthesizing low-dimensional cyanide-bridged magnetic complexes with various structure types, such as polynuclear, nano-size molecular wheels, or 1-D infinite chains. Chirality can be reasonably introduced into cyanide-bridged systems using the appropriate chiral ancillary ligand for coordination with paramagnetic ions. The optically active compound *S,S/R,R*-1,2-diphenylethylenediamine is a good chiral ligand and has been introduced into the field of cyanide-bridged magnetism system using its Schiff base manganese(III) complex as assembly segment [19b, 32]. However, there is no report to date about *S,S/R,R*-1,2-diphenylethylenediamine being used to prepare cyanide-bridged magnetic complexes. With this in mind, the reactions of *trans*-[Fe(bpb)(CN) $_2$] $^-$ with the chiral amine copper(II) compounds Cu[(*S,S/R,R*-dpen) $_2$](ClO $_4$) $_2$ were investigated, and three pairs of chiral cyanide-bridged Fe(III)–Cu(II) enantiomeric complexes have been obtained.

Table 1. Crystallographic data for 1–6.

	1	2	3	4	5	6
Chemical formula	C ₁₀₀ H ₉₇ Cl ₂ Cu ₂ Fe ₂ N ₂₂ O _{13.5}	C ₉₈ H ₁₀₂ Cl ₂ Cu ₂ Fe ₂ N ₂₀ O ₁₇	C ₅₂ H ₅₇ ClCuFeN ₁₁ O ₉	C ₄₉ H ₅₄ ClCuFeN ₁₀ O ₁₀	C ₅₃ H ₅₉ ClCuFeN ₁₁ O ₉	C ₅₃ H ₅₉ ClCuFeN ₁₁ O ₉
Fw	2132.67	2141.67	1134.93	1097.85	1148.95	1148.95
Crystal system	Triclinic	Triclinic	Orthorhombic	Orthorhombic	Orthorhombic	Orthorhombic
Space group	P1	P1	P212121	P212121	P212121	P212121
<i>a</i> (Å)	12.8309(4)	12.8039(6)	11.597(4)	11.441(5)	11.6020(4)	11.6593(12)
<i>b</i> (Å)	14.5164(6)	14.5907(6)	15.816(5)	15.641(7)	15.7614(6)	15.830(2)
<i>c</i> (Å)	16.1963(11)	16.2929(8)	29.855(10)	29.554(12)	29.9886(13)	29.993(3)
α (°)	111.243(5)	111.796(4)	90	90	90	90
β (°)	100.341(4)	100.649(4)	90	90	90	90
γ (°)	95.086(3)	94.546(4)	90	90	90	90
<i>V</i> (Å ³)	2726.9(2)	2740.8(2)	5476(3)	5289(4)	5483.8(4)	5535.7(11)
<i>Z</i>	1	1	4	4	4	4
Completeness	99.3%	99.5%	99.8%	99.8%	99.6%	99.2%
<i>F</i> (0 0 0)	1108	1108	2360	2320	2392	2392
θ (°)	3.05–25.01	3.16–25.01	1.88–25.01	1.90–25.01	2.98–25.00	2.91–25.01
GOF	1.048	1.034	1.030	1.029	1.003	0.994
<i>R</i> ₁ [<i>I</i> > 2(<i>I</i>)]	0.0698	0.0686	0.0487	0.0561	0.0537	0.0829
<i>wR</i> ₂ (all data)	0.2195	0.2141	0.1314	0.1505	0.1401	0.1960

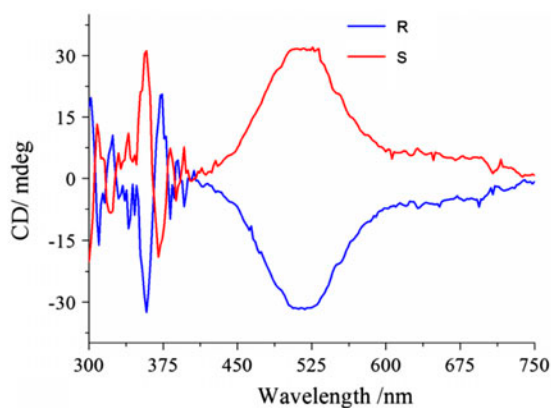


Figure 1. CD spectra of **1** (S isomer, red) and **2** (R isomer, blue) in KBr pellets (see <http://dx.doi.org/10.1080/00958972.2015.1080360> for color version).

Table 2. Selected bond lengths (Å) and angles (°) for **1**, **3**, and **5**.

	1	3	5
Cu1–N1	2.202(12)	2.218(3)	2.218(4)
Cu1–N7	2.011(11)	2.020(4)	2.029(5)
Cu1–N8	1.991(10)	2.031(4)	2.017(5)
Cu1–N9	2.024(12)	2.016(4)	2.022(5)
Cu1–N10	1.980(11)	2.042(4)	2.039(5)
Fe1–C1	1.994(15)	1.991(4)	1.996(5)
Fe1–C2	1.918(13)	1.974(4)	1.972(4)
Fe1–N3	1.865(10)	1.898(5)	1.896(5)
Fe1–N4	1.898(11)	1.905(5)	1.887(5)
Fe1–N5	2.011(10)	2.003(4)	2.006(5)
Fe1–N6	1.998(10)	2.013(4)	2.006(5)
Cu1–N1–C1	165.9(12)	175.2(3)	175.4(4)
Fe1–C1–N1	172.8(12)	178.6(5)	179.0(5)
Fe1–C2–N2	176.3(11)	177.2(5)	177.0(6)

The cyanide-bridged complexes have been characterized by IR spectroscopy. In the IR spectra of **1–6**, two sharp peaks due to the cyanide-stretching vibrations were observed near 2125–2130 and 2155–2160 cm^{-1} , respectively, indicating the presence of bridging and non-bridging cyanide ligands in these complexes. The strong broad peak near 1100 cm^{-1} is attributed to free ClO_4^- . The optical activity and enantiomeric nature for the above six complexes has been further confirmed by circular dichroism (CD) spectroscopy in KBr pellets with **1** and **2** as representative. As can be seen in figure 1, the CD spectra of **1** (S isomer) and **2** (R isomer) exhibit positive and negative cotton effects at similar wavelengths.

3.2. Crystal structures of **1–6**

Some important structural parameters for **1**, **3**, and **5** are collected in table 2. The perspective view of the enantiomeric structure of (**1**, **2**), (**3**, **4**), and (**5**, **6**) is shown in figures 2–4, respectively. The cell packing diagram for these six complexes (with **1** as a representative) is given in figure 5.

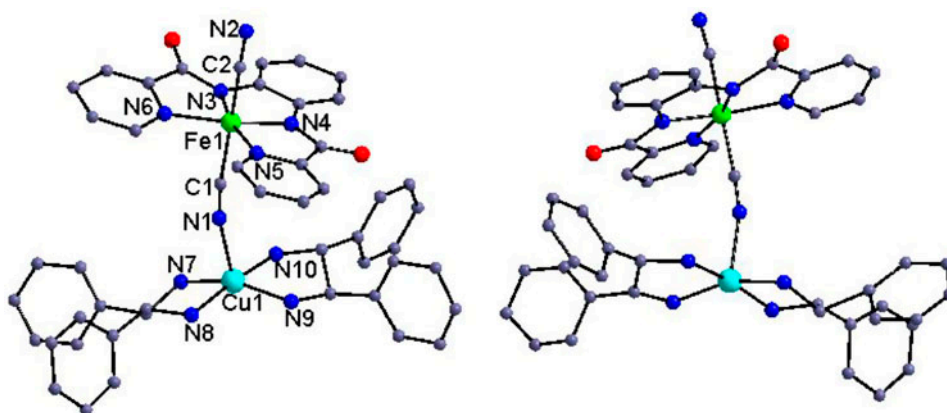


Figure 2. Perspective view of the cationic structure of **1** (S,S isomer, left) and **2** (R,R isomer, right), respectively. All the hydrogens, the balanced anion, and the solvent molecules have been omitted for clarity.

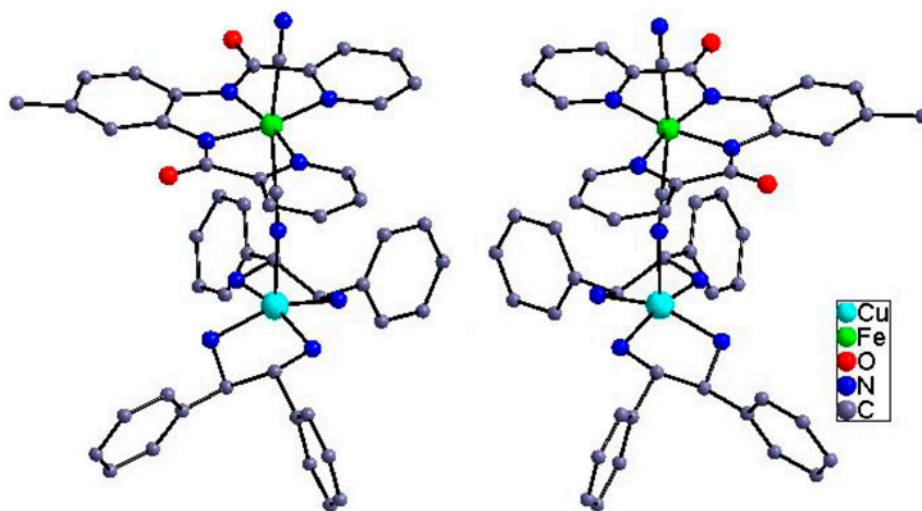


Figure 3. Perspective view along the *a* axis of the cationic structure of **3** (S,S isomer, left) and **4** (R,R isomer, right), respectively. All the hydrogens, the balanced anion, and the solvent molecules have been omitted for clarity.

As can be seen from figures 2–4, the complexes (**1**, **2**), (**3**, **4**), and (**5**, **6**) are three pairs of enantiomers, respectively. Therefore, complexes **1**, **3**, and **5** will be used as examples for the description of the structures for **1**–**6**. This series of complexes forms cationic cyanide-bridged binuclear structures with free ClO_4^- ions balancing the charge. In all the complexes, each cyanide-containing building block is a monodentate ligand through one of its two *trans* cyanide groups toward Cu(II). The Fe(III) is six-coordinate with four equatorial nitrogens from the pyridinecarboxamide ligand and two carbons from the two cyanide groups with a *trans* orientation, forming a slightly distorted octahedral geometry, which can be shown by the bond parameters around the Fe(III) ion (table 2). The Fe–C≡N bond angle is 172.8(12)–179.0(5)° and clearly indicates that the three atoms are in a nearly linear alignment.

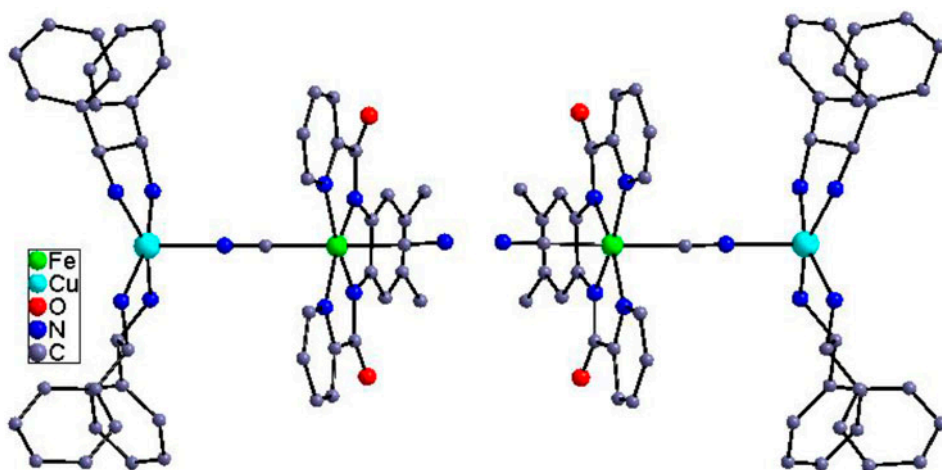


Figure 4. Perspective view along the a axis of the cationic structure of **5** (S,S isomer, left) and **6** (R,R isomer, right), respectively. All the hydrogens, the balanced anion, and the solvent molecules have been omitted for clarity.

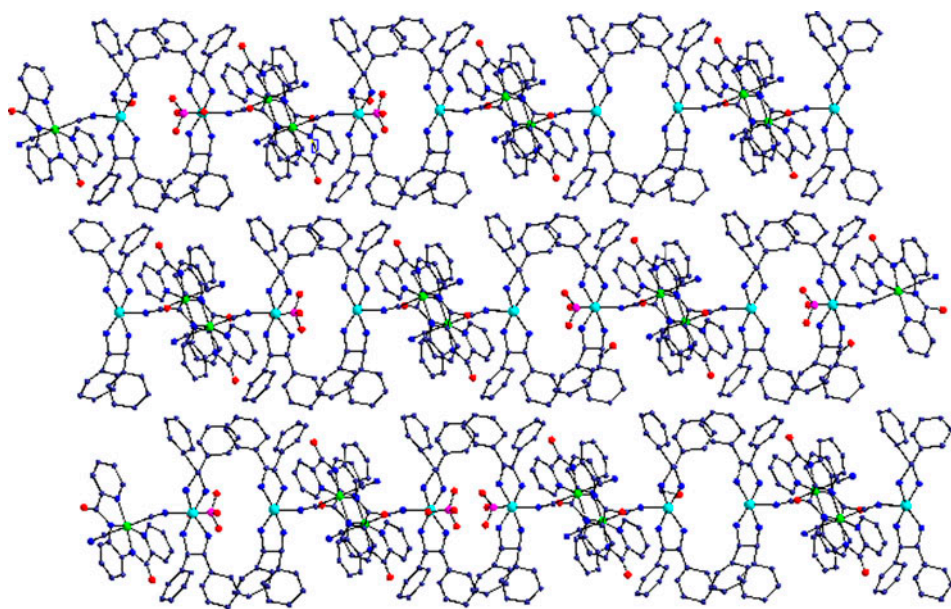


Figure 5. The representative cell packing along the c axis for **1–6**. The solvent molecules and all the hydrogens have been omitted for clarity.

The Cu ion in **1**, **3**, and **5** is five-coordinate, with four nitrogens from amine ligands and the additional one from the bridging cyanide of the *trans*-dicyanometalate. The Cu ion is only out of the plane formed by four N atoms of the amine molecules by 0.25(1), 0.33(9), and 0.34(3) Å toward the coordinated N_{cyanide} in **1**, **3**, and **5**, respectively. According to Addison's method for calculating the geometry of five-coordinate Cu(II) structures [33], the τ value defined as $(\beta - \alpha)/60^\circ$, in which β and α represent the two larger basal angles, is

0.25, 0.16, and 0.11 for **1**, **3**, and **5**, respectively, giving further evidence that the Cu(II)-geometry is more square pyramidal than trigonal-bipyramidal. The average Cu–N_{amine} bond lengths in these three complexes are 2.007, 2.026, and 2.027 Å, respectively, obviously shorter than the Cu–N_{cyanide} bond length with values of 2.202(12), 2.218(3), and 2.218(4) Å, clearly showing the markedly distorted square pyramidal geometry of Cu(II). The C≡N–Cu bond angles in **1–3** are 165.9(12), 175.2(3), and 175.4(4)°, respectively, demonstrating that these three atoms are also approaching linear, and also giving information that the substituent group on the cyanide precursor has influence on the configuration of the C≡N–Cu bond angle. The intramolecular Fe^{III}–Cu^{II} separation through bridging cyanide is 5.256, 5.351, and 5.352 Å for **1**, **3**, and **5**, respectively, which are obviously shorter than the shortest intermolecular metal–metal distance with the values of 7.014, 6.556, and 6.535 Å.

4. Magnetic properties of **1**, **3**, and **5**

The temperature dependences of the magnetic susceptibilities measured from 2 to 300 K in an applied field of 2000 Oe for **1**, **3**, and **5** are given in figure 6. The room temperature $\chi_m T$ values of **1**, **3**, and **5** are 0.855, 0.865, and 0.895 emu K mol⁻¹, respectively, higher than the spin-only value of 0.75 emu K mol⁻¹ expected for one isolated Cu^{II} and one low-spin Fe^{III} ($S = 1/2$) assuming $g = 2.0$, which is likely due to the orbital contribution to the magnetic moment of the low-spin Fe^{III}. As can be found from figure 6, the general shapes of

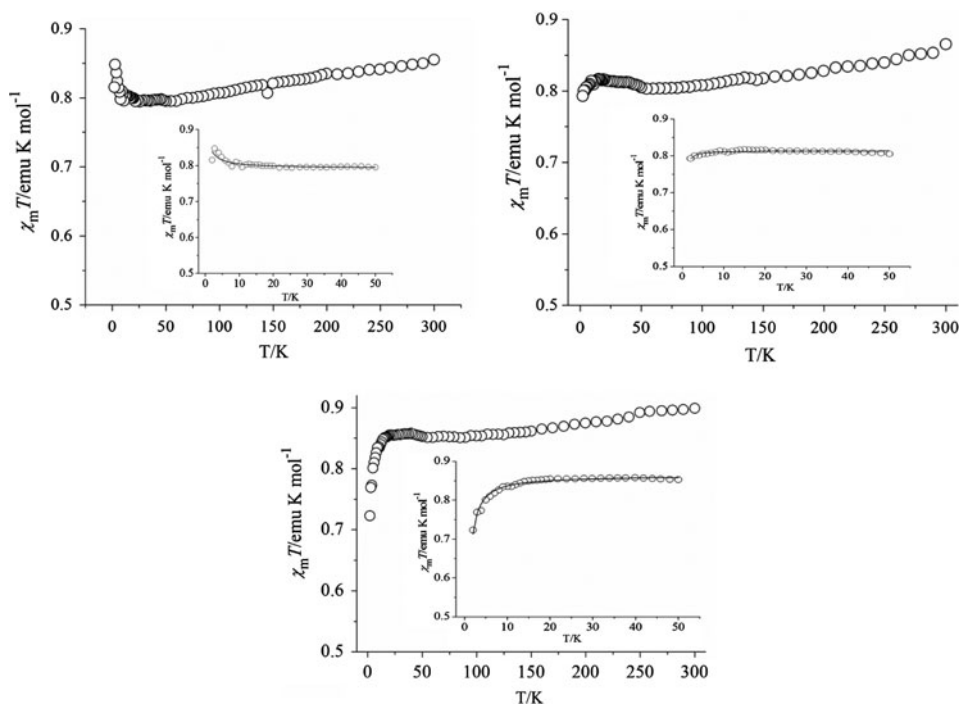


Figure 6. Temperature dependences of $\chi_m T$ and χ_m^{-1} for **1** (top, left), **3** (top, right), and **5** (bottom) (the solid line for $\chi_m T$ represents the best fit based on the parameters discussed in the text).

the $\chi_m T$ - T curves for these three complexes are similar, and the $\chi_m T$ value decreases smoothly with temperature from room temperature to about 50 K. Such magnetic behavior is characteristic of a low-spin octahedral iron(III) system with spin-orbit coupling of the ${}^2t_{2g}$ ground term. A similar temperature dependence of $\chi_m T$ has been observed for a compound containing only paramagnetic $[\text{Fe}(\text{CN})_6]^{3-}$ ions [34]. On further lowering the temperature, the $\chi_m T$ value initially begins to increase and then decreases with temperature down to 2 K. The increase in $\chi_m T$ at low temperature is consistent with weak ferromagnetic coupling between Fe(III) and Cu(II) spins, which is similar to the results demonstrated in Fe(III)Cu(II) or M(V)Cu(II) (M=Mo, W) bimetallic systems bearing axially elongated Cu(II) ions [34–39]. Due to the orbital contribution from the low-spin Fe(III) ion, the magnetic fitting from 2 to 300 K for these three complexes failed to give satisfactory results. To further confirm the ferromagnetic coupling nature between the cyanide-bridged Fe(III)–Cu(II), the magnetic susceptibilities of **1**, **3**, and **5** from 2 to 50 K were analyzed with Fe–Cu dinuclear magnetic model based on the exchange spin Hamiltonian $H = -2J S_{\text{Fe}} S_{\text{Cu}}$:

$$\chi_d = \frac{Ng^2\beta^2}{3kT} \left[1 + \frac{1}{3} \exp \frac{J}{kT} \right]^{-1}$$

$$\chi_m = \frac{\chi_d}{1 - \chi_d(2zJ'Ng^2\beta^2)}$$

where N is Avogadro's number, g is the electronic g factor, β is the Bohr magneton, k is the Boltzmann constant, T is the absolute temperature, zJ' is the intermolecular magnetic interaction. Using the above model, the susceptibilities over the temperature range of 2–50 K for these three complexes were simulated, giving the best-fit parameters $J = 0.71(1) \text{ cm}^{-1}$, $g = 2.15(2)$, $zJ' = -0.22(2) \text{ cm}^{-1}$, $R = \sum(\chi_{\text{obsd}}T - \chi_{\text{calcd}}T)^2 / \sum(\chi_{\text{obsd}}T)^2 = 2.90 \times 10^{-5}$ for **1**, $J = 0.37(2)$, $g = 2.10(8)$, $zJ' = -0.48(5) \text{ cm}^{-1}$, $R = 3.29 \times 10^{-5}$ for **3**, and $J = 0.31(3)$, $g = 2.12(1)$, $zJ' = -0.43(2) \text{ cm}^{-1}$, $R = 4.99 \times 10^{-5}$ for **5**, which further support the weak ferromagnetic exchange between the low-spin Fe(III) ion and the Cu(II) ion through the bridging cyanide.

Figure 7 shows the field-dependent magnetization measured up to 50 kOe at 2 K for **1**, **3**, and **5**, and their χ_m^{-1} - T curves are given in the corresponding inset. The Brillouin curve is drawn based on uncoupled low-spin Fe(III) and Cu(II) spins. By careful examination of the field-dependent magnetization in the low field range, one can see that the experimental data reside slightly higher than the calculated plot, especially for **1**, demonstrating the operation of overall weak ferromagnetic interactions.

As shown previously, due to the strict orthogonality of the magnetic orbitals, the observed ferromagnetic coupling between nearest paramagnetic neighbors in linear cyanide-bridged systems is commonly found. The electronic configuration of low-spin Fe(III) is $t_{2g}^5 e_g^0$ with the unpaired electron occupying one of the three t_{2g} orbital. The copper(II) ion is a Jahn–Teller-active metal ion with the electronic configuration $t_{2g}^6 e_g^3$ and tends to afford short, strong equatorial bonds and long, weak bonds to the terminal N of the bridging cyanide ligands. Furthermore, as discussed above, the Cu ion and the bridging cyanide group are in a nearly linear conformation with the Cu–N≡C bond angles close to 180°. Therefore, the universal ferromagnetic coupling observed in this series of cyanide-bridged

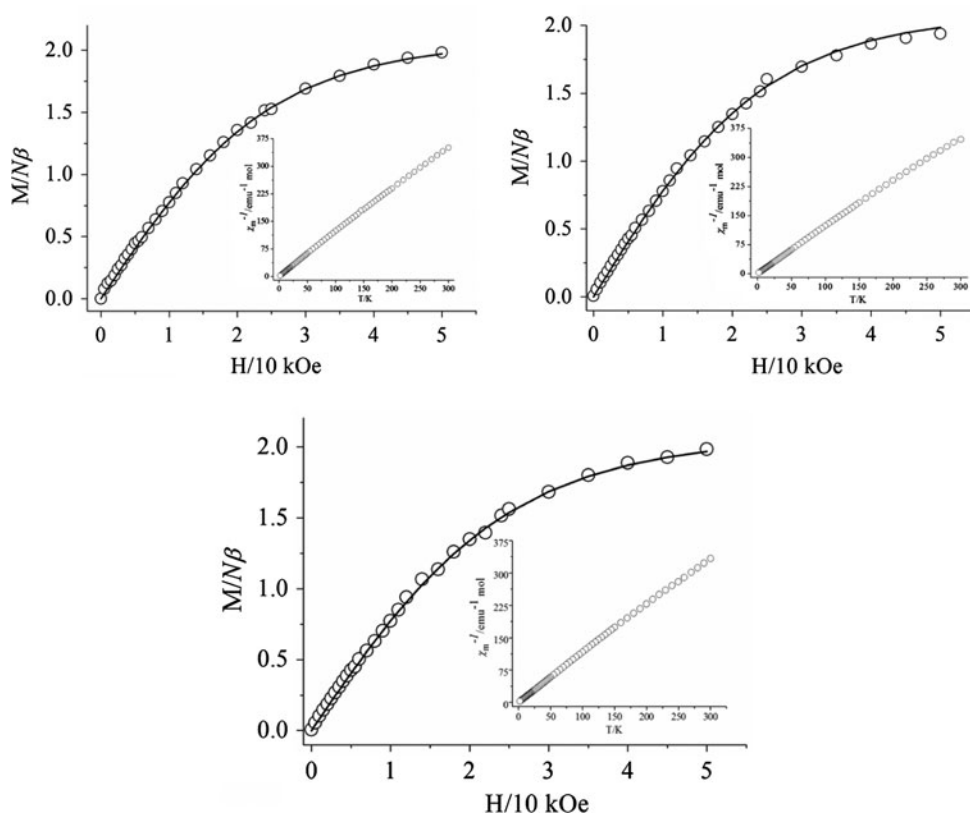
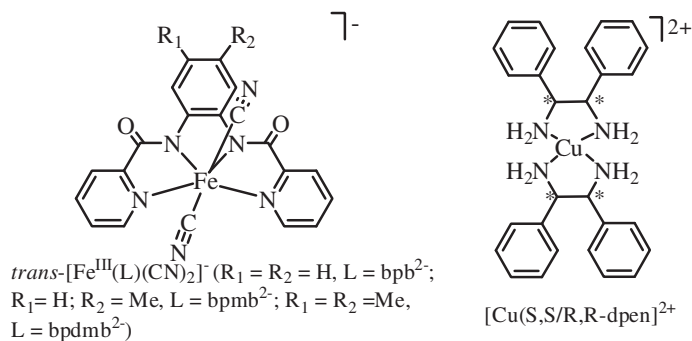


Figure 7. Field dependence of magnetization at 2 K (the line is the Brillouin curve for uncoupled low-spin Fe(III) ($S = 1/2$) and Cu(II) ($S = 1/2$) with $g = 2.0$) for **1** (top, left), **3** (top, right), and **5** (bottom). Inset: The $\chi_m^{-1}-T$ curve for the corresponding complex.



Scheme 1. The starting materials used.

Fe(III)–Cu(II) examples can be easily interpreted by the orthogonality of the t_{2g} magnetic orbital of Fe(III) ion with the e_g orbital of the Cu(II) ion through a linear cyanide bridge.

5. Conclusion

A series of chiral cyanide-bridged heterobimetallic binuclear Fe(III)–Cu(II) complexes have been designed and synthesized based on chiral amine copper(II) compounds using three *trans*-dicyanideiron(III)-containing building blocks $K[Fe(L)(CN)_2]$. The formation of only bimetallic systems, but not trinuclear ones or 1D-chains can be attributed to the comparatively large steric effect from the organic amine ligand. Investigation of their magnetic properties reveals an overall weak ferromagnetic interaction between the cyanide-bridged Fe–Cu metal centers.

Supplementary material

CCDC 1048994-1048999 contain the supplementary crystallographic data for complexes **1–6**. These data can be obtained free of charge via <http://www.ccdc.ac.uk/conts/retrieving.html>, or from the Cambridge Crystallographic Data Center, 12 Union Road, Cambridge CB21EZ, UK; fax:+44 1223 336 033; or e-mail: deposit@ccdc.cam.ac.uk.

Disclosure statement

No potential conflict of interest was reported by the authors.

Funding

This work was supported by the National Natural Science Foundation of China [grant number 21171107]; Natural Science Foundation of Shandong Province [grant number ZR2011BM008]; Science and Technology Project of High Education, Shandong Province [grant number J11LB09].

References

- [1] M.M. Turnbull, T. Sugimoto, L.K. Thompson. *Molecule-based Magnetic Materials*, American Chemical Society, Washington, DC (1996).
- [2] J.S. Miller, D. Gatteschi. *Chem. Soc. Rev.*, **40**, 3065 (2011).
- [3] M. Mannini, F. Pineider, P. Sainctavit, C. Danieli, E. Otero, C. Sciancalepore, A.M. Talarico, M.A. Arrio, A. Cornia, D. Gatteschi, D. Sessoli. *Nat. Mater.*, **8**, 194 (2009).
- [4] M. Mannini, F. Pineider, C. Danieli, F. Totti, L. Sorace, P. Sainctavit, M.A. Arrio, E. Otero, L. Joly, J.C. Cezar, A. Cornia, R. Sessoli. *Nature*, **468**, 417 (2010).
- [5] (a) H. Miyasaka, A. Saitoh, S. Abe. *Coord. Chem. Rev.*, **251**, 2622 (2007); and references therein; (b) K.R. Dunbar, R.A. Heintz. *Prog. Inorg. Chem.*, **57**, 155 (2009).
- [6] (a) S. Wang, X.H. Ding, J.L. Zuo, X.Z. You, W. Huang. *Coord. Chem. Rev.*, **255**, 1713 (2011); (b) S. Wang, X.H. Ding, Y.H. Li, W. Huang. *Coord. Chem. Rev.*, **256**, 439 (2012); (c) Y.H. Li, W.R. He, X.H. Ding, S. Wang, L.F. Cui, W. Huang. *Coord. Chem. Rev.*, **256**, 2795 (2012).
- [7] (a) T. Senapati, C. Pichon, R. Ababei, C. Mathonière, R. Clérac. *Inorg. Chem.*, **51**, 3796 (2012); (b) A. Panja, P. Guionneau, I.R. Jeon, S.M. Holmes, R. Clérac, C. Mathonière. *Inorg. Chem.*, **51**, 12350 (2012).
- [8] (a) W.R. Entley, G.S. Girolami. *Science*, **268**, 397 (1995); (b) O. Sato, T. Iyoda, A. Fujishima, K. Hashimoto. *Science*, **271**, 49 (1996).
- [9] (a) Ø. Hatlevik, W.E. Buschmann, J. Zhang, J.L. Manson, J.S. Miller. *Adv. Mater.*, **11**, 914 (1999); (b) Z. Lv, X. Wang, Z. Liu, F. Liao, S. Gao, R. Xiong, H. Ma, D. Zhang, D. Zhu. *Inorg. Chem.*, **45**, 999 (2006).

- [10] J.M. Herrera, V. Marvaud, M. Verdaguer, J. Marrot, M. Kalisz, C. Mathonière. *Angew. Chem. Int. Ed.*, **43**, 5468 (2004).
- [11] (a) J. Long, L.M. Chamoreau, C. Mathonière, V. Marvaud. *Inorg. Chem.*, **47**, 22 (2008); (b) A. Bleuzen, V. Marvaud, C. Mathonière, B. Sieklucka, M. Verdaguer. *Inorg. Chem.*, **48**, 3453 (2009).
- [12] J.S. Miller, M. Drillon (Eds.). *Magnetism – Molecules to Materials*, Vols. 1–5, Wiley-VCH, Mannheim (2001–2005).
- [13] (a) J.A. Rodríguez-Velamazán, M.A. González, J.A. Real, M. Castro, M.C. Muñoz, A.B. Gaspar, R. Ohtani, M. Ohba, K. Yoneda, Y. Hijikata, N. Yanai, M. Mizuno, H. Ando, S. Kitagawa. *J. Am. Chem. Soc.*, **134**, 5083 (2012); (b) F.J. Muñoz-Lara, A.B. Gaspar, D. Aravena, E. Ruiz, M.C. Muñoz, M. Ohba, R. Ohtani, S. Kitagawa, J.A. Real. *Chem. Comm.*, **48**, 4686 (2012); (c) C. Bartual-Murgui, L. Salmon, A. Akou, N.A. Ortega-Villar, H.J. Shepherd, M.C. Muñoz, G. Molnár, J.A. Real, A. Bousseksou. *Chem. Eur. J.*, **18**, 507 (2012).
- [14] (a) I.R. Jeon, S. Calancea, A. Panja, D.M. Piñero Cruz, E.S. Koumoussi, P. Dechambenoit, C. Coulon, A. Wattiaux, P. Rosa, C. Mathonière, R. Clérac. *Chem. Sci.*, **4**, 2463 (2013); (b) T. Shiga, G.N. Newton, J.S. Mathieson, T. Tetsuka, M. Nihei, L. Cronin, H. Oshio. *Dalton Trans.*, **39**, 4730 (2010).
- [15] (a) Z. Smékal, T. Maris, M. Korabik. *J. Coord. Chem.*, **67**, 3167 (2014); (b) Ş.A. Korkmaz, A. Karadağ, N. Korkmaz, Ö. Andaç, N. Gürbüz, İ. Özdemir, R. Topkaya. *J. Coord. Chem.*, **66**, 3072 (2013); (c) A. Karadağ, Ş.A. Korkmaz, Ö. Andaç, Y. Yerli, Y. Topcu. *J. Coord. Chem.*, **65**, 1685 (2012); (d) Y.M. Gayfulin, A.I. Smolentsev, Y.V. Mironov. *J. Coord. Chem.*, **64**, 3832 (2011); (e) K.R. Ranjan, A. Singh, A. Banerjee, B. Singh. *J. Coord. Chem.*, **64**, 805 (2011); (f) A. Panja. *J. Coord. Chem.*, **64**, 987 (2011).
- [16] (a) N. Hoshino, Y. Sekine, M. Nihei, H. Oshio. *Chem. Commun.*, **46**, 6117 (2010); (b) Y.Y. Zhu, X. Guo, C. Cui, B.W. Wang, Z.M. Wang, S. Gao. *Chem. Commun.*, **47**, 8049 (2011).
- [17] M. Gruselle, C. Train, K. Boubekour, P. Gredin, N. Ovanesyan. *Coord. Chem. Rev.*, **250**, 2491 (2006).
- [18] (a) C.M. Liu, R.G. Xiong, D.Q. Zhang, D.B. Zhu. *J. Am. Chem. Soc.*, **132**, 4044 (2010); (b) Y.Z. Zhang, O. Sato. *Inorg. Chem.*, **49**, 1271 (2010); (c) D.P. Zhang, Y.Z. Bian, J. Qin, P. Wang, X. Chen. *Dalton Trans.*, **43**, 945 (2014).
- [19] (a) D.E. Freedman, D.M. Jenkins, A.T. Iavarone, J.R. Long. *J. Am. Chem. Soc.*, **130**, 2884 (2008); (b) M.X. Yao, Q. Zheng, X.M. Cai, Y.Z. Li, Y. Song, J.L. Zuo. *Inorg. Chem.*, **51**, 2140 (2012); (c) J. Ru, F. Gao, T. Wu, M.X. Yao, Y.Z. Li, J.L. Zuo. *Dalton Trans.*, **43**, 933 (2014).
- [20] (a) E.J. Schelter, A.V. Prosvirin, W.M. Reiff, K.R. Dunbar. *Angew. Chem. Int. Ed.*, **43**, 4912 (2004); (b) Z.H. Ni, H.Z. Kou, L.F. Zhang, C. Ge, A.L. Cui, R.J. Wang, Y. Li, O. Sato. *Angew. Chem. Int. Ed.*, **45**, 7742 (2005).
- [21] (a) J.P. Sutter, S. Dhers, R. Rajamani, S. Ramasesha, J.P. Costes, C. Duhayon, L. Vendier. *Inorg. Chem.*, **48**, 5820 (2009); (b) A.L. Goodwin, B.J. Kennedy, C. Kepert. *J. Am. Chem. Soc.*, **131**, 6334 (2009).
- [22] L.M. Toma, R. Lescouëzec, J. Pasán, C. Ruiz-Pérez, J. Vaissermann, J. Cano, R. Carrasco, W. Wernsdorfer, F. Lloret, M. Julve. *J. Am. Chem. Soc.*, **128**, 4842 (2006).
- [23] (a) S. Choi, H.Y. Kwak, J.H. Yoon, H.C. Kim, E.K. Koh, C.S. Hong. *Inorg. Chem.*, **47**, 10214 (2008); (b) H. Miyasaka, M. Julve, M. Yamashita, R. Clérac. *Inorg. Chem.*, **48**, 3420 (2009).
- [24] (a) T.D. Harris, M.V. Bennett, R. Clérac, J.R. Long. *J. Am. Chem. Soc.*, **132**, 3980 (2010); (b) D.P. Zhang, L.F. Zhang, Y.T. Chen, H.L. Wang, Z.H. Ni, W. Wernsdorfer, J.Z. Jiang. *Chem. Commun.*, **46**, 3550 (2010).
- [25] (a) Z.H. Ni, H.Z. Kou, L.F. Zhang, V. Tangoulis, W. Wernsdorfer, A.L. Cui, O. Sato. *Inorg. Chem.*, **46**, 6029 (2007); (b) Z.H. Ni, H.Z. Kou, Y.H. Zhao, L. Zheng, R.J. Wang, A.L. Cui, O. Sato. *Inorg. Chem.*, **44**, 2050 (2005); (c) Z.H. Ni, J. Tao, W. Wernsdorfer, A.L. Cui, H.Z. Kou. *Dalton Trans.*, **38**, 2788 (2009).
- [26] H.Z. Kou, Z.H. Ni, C.M. Liu, D.Q. Zhang, A.L. Cui. *New J. Chem.*, **33**, 2296 (2009).
- [27] (a) D.P. Zhang, H.L. Wang, Y.T. Chen, Z.H. Ni, L.J. Tian, J.Z. Jiang. *Inorg. Chem.*, **48**, 5488 (2009); (b) D.P. Zhang, L.F. Zhang, Z.D. Zhao, X. Chen, Z.H. Ni. *Inorg. Chim. Acta*, **377**, 165 (2011); (c) D.P. Zhang, Z.D. Zhao, P. Wang, Z.H. Ni. *CrystEngComm.*, **15**, 2504 (2013); (d) D.P. Zhang, W.J. Si, P. Wang, X. Chen, J.Z. Jiang. *Inorg. Chem.*, **53**, 3494 (2014).
- [28] M. Ray, R. Mukherjee, J.F. Richardson, R.M. Buchanan. *J. Chem. Soc., Dalton Trans.*, 2451 (1993).
- [29] Bruker APEX2 and SAINT- PLUS. *Bruker CCD X-ray Diffractometer Control*, Bruker AXS Inc., Madison, WI (2001/2004).
- [30] G.M. Sheldrick. *SADABS*, University of Göttingen, Göttingen (2012).
- [31] G.M. Sheldrick. *Acta Cryst.*, **A64**, 112 (2008).
- [32] J. Ru, F. Gao, M.X. Yao, T. Wu, J.L. Zuo. *Dalton Trans.*, **43**, 18047 (2014).
- [33] A.W. Addison, T.N. Rao. *J. Chem. Soc., Dalton Trans.*, 1349 (1984).
- [34] A. Rodríguez-Diéguez, R. Kivekäs, R. Sillanpää, J. Cano, F. Lloret, V. McKee, H. Stoeckli-Evans, E. Colacio. *Inorg. Chem.*, **45**, 10537 (2006).
- [35] J.M. Lim, Y.S. You, H.S. Yoo, J.H. Yoon, J.I. Kim, E.K. Koh, C.S. Hong. *Inorg. Chem.*, **46**, 10578 (2007).
- [36] M. Atanasov, P. Comba, C.A. Daul. *J. Phys. Chem. A*, **110**, 13332 (2006).
- [37] J.H. Lim, J.H. Yoon, S.Y. Choi, D.W. Ryu, E.K. Koh, C.S. Hong. *Inorg. Chem.*, **50**, 1749 (2011).
- [38] E. Colacio, J.M. Domínguez-Vera, M. Ghazi, R. Kivekäs, J.M. Moreno, A. Pajunen. *J. Chem. Soc., Dalton Trans.*, 505 (2000).
- [39] (a) D.P. Zhang, S.P. Zhuo, P. Wang, X. Chen, J.Z. Jiang. *New J. Chem.*, **38**, 5470 (2014); (b) D.P. Zhang, L.Q. Kong, Z.D. Zhao, P. Wang, X. Chen. *Transition Metal Chem.*, **39**, 337 (2014).